Formation of Field-Reversed Configuration by Larger Rotating Magnetic Field

M.Ohnishi,[1] T.Chikano,[1] M.Tsukamoto,[1] M.Fukuhara,[1] T.Masaki,[1] H.Osawa,[1] W.Hugrass,[2]
Kansai University,[1] University of Tasmania[2]

(Received: 3 September 2008 / Accepted: 14 December 2008)

A Field-Reversed Configuration (FRC) is formed by applying Rotating Magnetic Field (RMF) much larger than the axial magnetic field to a cylindrical glass vacuum chamber filled with 10Pa Argonne gas without a pre-ionization. The FRC with the plasma density $2.2\times10^{19}\mathrm{m}^{-3}$, the temperature 8.0eV, the separatrix length 0.45m and the separatrix radius 0.035m is sustained for the notably long period 40msec. During the period the RMF is fully penetrated into the center and drives the current with peaked profile near the field null. The θ-component of RMF plays a major role in a radial force balance between the plasma pressure and the magnetic pressure.

Keywords: Field-Reversed Configuration (FRC), Rotating Magnetic Field (RMF), current drive, penetration of RMF

1. Introduction

A rotating magnetic field (RMF) has been used for the purpose of the slow formation and the sustainment of a Field-Reversed Configuration (FRC) [1-7]. When the RMF frequency satisfies that $\omega_{ci}\leq\omega\ll\omega_{ce}$ and $\nu_{ei}\ll\omega_{ce}$ [4], where ω_{ci} and ω_{ce} are the cyclotron frequency of ions and electrons for RMF and ν_{ei} the electron ion collision frequency, it is proven that the RMF drives the current and forms FRC's which possess the temperature about 10-100eV, and the density about 10^{18}-10^{19} m^{-3} [7]. The most of previous devices first ionize the neutral gas with low pressure about 0.05 Pa by an RF power and apply the RMF. When the condition $\omega_{ce}/\nu_{ei}>R/\delta$ is roughly satisfied where R the separatrix radius and δ the classical skin depth given by $\delta=(2\eta/\mu_0\omega)^{1/2}$, the RMF penetrates into the plasma.[8] The application of an RMF makes it possible, in principle, to sustain the FRC indefinitely. In practice, the life of an FRC is at most several msec due to the restriction of the capability of power supply.[2,3] The effect of the RMF on the pressure balance equations was assumed negligible in the early theoretical investigations[9,10] and this assumption was verified by detailed measurements of the magnetic field, plasma density and temperature[11].

There have not been any experiments where the RMF is much larger than the axial magnetic field. We apply RMF much larger than the axial magnetic field to the glass vacuum chamber filled with 10Pa Argonne gas without pre-ionization. The purposes of the study are to examine the effects of larger RMF on the radial force balance of FRC sustained by an RMF, and to investigate the penetration of the RMF much larger than the axial field.

e-mail address:onishi@kansai-u.ac.jp

2. Experimental Set-up

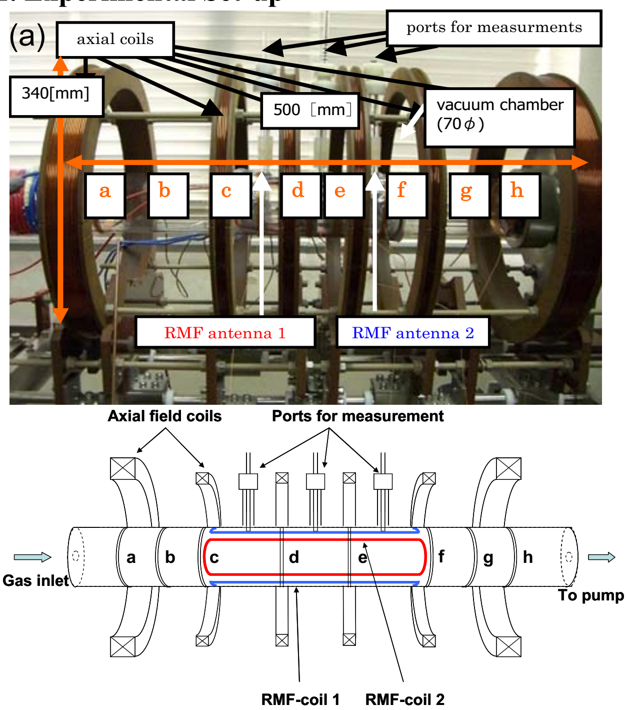

Fig.1 Experimental Device. (a) photo of facility and (b) schematic diagram

Figure 1 shows the photo and schematic diagram of the experimental device. The cylindrical vacuum chamber is made of Pyrex glass and has an internal radius of 35mm. The length of the discharge chamber is 600mm. The vacuum is achieved to be less than 10^{-4} Pa in ten minutes by a rotary pump and a turbo molecular pump in a series. Argonne gas is fed from the opposite side to the vacuum pumping system. The axial field is produced by 6 coils and the strength is fairly uniform along the central axis and 60 Gauss at the maximum. Two RMF power supplies, of which sinusoidal output is 90 degree out of phase, deliver the current 300 A, the frequency 200 kHz and out put power 13 kW for the period 40msec each. The current decrease to 200 A at t=40msec by the limited capacity of the condenser. The antennas are wound by two turn in touch with the chamber in order to produce the largest RMF inside the chamber. The amplitude of the RMF is initially 120 Gauss at the center and reduces to 80 Gauss at t=40msec due to the decrease of the antenna current. The production of current in the antenna uses a resonance circuit in R-L-C series and insulated gate bipolar transistor semiconductor switching devices.

3. Experimental Results

3.1. Magnetic field measurement

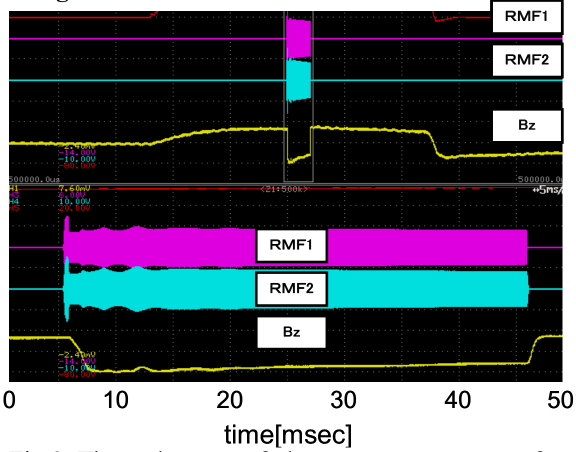

Fig.2 Time changes of the antenna currents of RMF1 and RMF2, and axial magnetic field Bz. The lower figures are enlarged to see the detailed behavior of the antenna currents and the axial field

Figure 2 shows the time changes of the antenna currents of RMF1 and RMF2, the axial magnetic field at the center of the chamber, and the enlargement of those values. The axial field slowly rises and reaches 25 Gauss. At the instance of applying the RMF, the axial field reduces to about -24 Gauss at the center (r=0, z=0) to 26.5 Gauss at the wall (r=35mm, z=0). The reversed field gradually reduces as the antenna current decreases. The behaviors are more apparently seen in the lower enlarged figures. The current is initially 300A for 500μsec and reduced to 155A after a plasma is formed. It takes 1.5msec for the axial field to be reversed. The antenna currents as well as the reversed field fluctuate for 15msec, and follow a slowly decreasing but quiet phase. The fluctuation cannot be explained, but it is supposed to be related to the intermediate time scale relaxation process described by L. Steinhauer.[12]

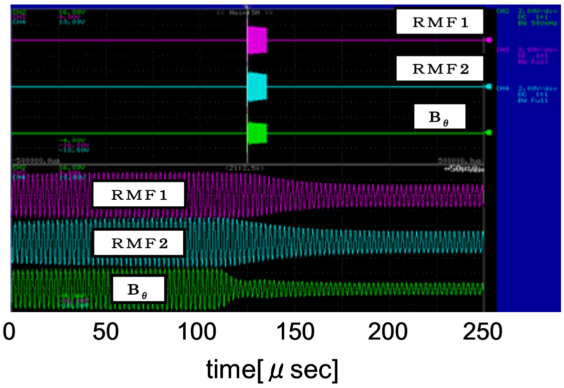

Fig.3 Antenna currents and the θ-component of RMF. The lower figures shows the antenna currents and the θ-component of the RMF at the instance of the plasma formation

Figure 3 shows the antenna currents and the θ-component of RMF in the center. The lower curves shows the enlarged ones about the instance of the plasma formation. The RMF reduces less than half, but still exists in the center, which shows the RMF continues to penetrate into the center after the formation of the FRC. The reduction of the antenna current may be caused both by an increase in the antenna resistance and by being out of a resonant condition due to the decrease in the inductance.[14]

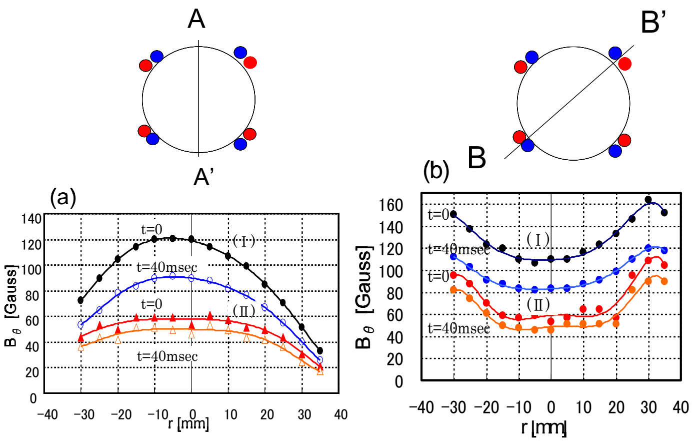

Fig.4 Radial profiles of the θ-component of the RMF. (a) and (b) show the profiles along the lines A-A' and B-B', respectively.

Figure 4 (a) and (b) show the radial dependence of the θ-component of the RMF along the line A-A' and B-B', respectively. (I) and (II) indicate the absence and the existence of a plasma. The magnitudes of the RMF along the line A-A' in a vacuum are peaked at the center, but get lower and fairy flat at the plasma existence. On the other hand, the magnitude along the line B-B' takes a minimum at the center and increases outward. The plasma existence similarly reduces the magnitude, which is still concave downwards. The difference of the magnitudes of the field between at t=0 and t=40msec is large at the absence of plasma, but it is much less at the existence of a plasma. The RMF is appreciably shielded by the FRC plasma, but the RMF still deeply penetrates into the plasma.

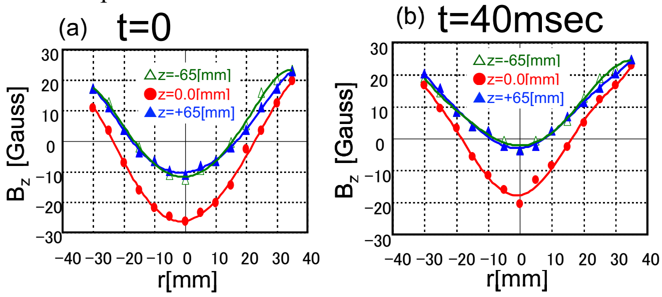

Fig.5 Radial profiles of axial magnetic field at the three position of the center axis. (a) and (b) correspond t=0 and t=40msec, respectively

Figures 5 (a) and (b) show the radial profiles of the axial magnetic field at the three axial positions z=0 and ±65mm at the instances t=0 and t=40msec, respectively. The field null point moves from 23mm to 18mm at z=0, and 18mm to 5mm at z=±65 during the discharge. At t=40msec, the RMF preserves barely the FRC although the field null radius becomes smaller.

Figure 6 shows the magnetic flux evaluated by using the results shown in Fig.5. The separatrix is identified by the cross point of the curves across the horizontal line, i.e. Ψ=0. The separatrix radius is r=35mm at z=0, and r=25mm at z=65mm. As time goes on, the radius of the separatrix decreases. Figure 7 shows the current profiles calculated by the axial magnetic profiles at t=0sec. The currents do not stand for a rigid rotor profile, but rather a peaked profile near the field null.

The separatrix length is measured by the coil wound on the glass chamber at 8 axial positions from a to h as shown in Fig.1(b). The separatrix length, then, is supposed to be about 330mm. The antenna length, incidentally, is 220mm.

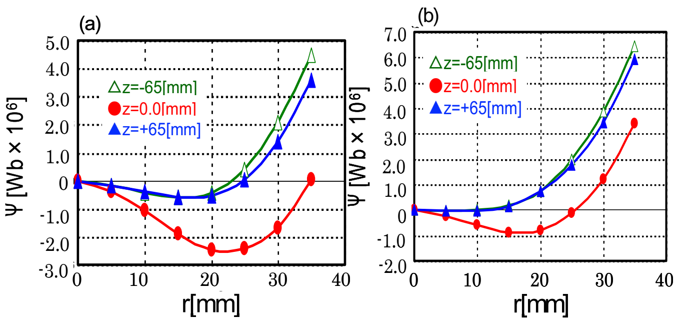

Fig.6 Magnetic flux profiles at the three position on the center axis. (a) and (b) are the values at t=0 and t=40msec

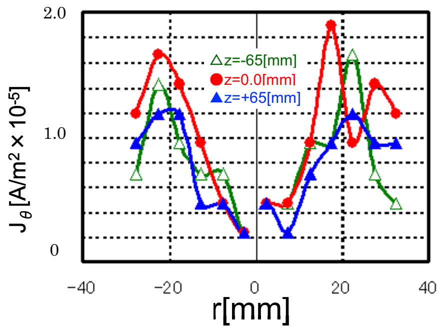

Fig.7 Current profiles evaluated from Fig.5(a)

3.2. Plasma density and electron temperature

The plasma density and electron temperature are measured by a double probe at t=20msec, when the FRC is in a quiet phase. Figure 8 (a) and (b) show the radial profiles of the electron temperature and the plasma density, respectively. The hollow temperature profile is consistent with the current density profile shown in figure 7. It is also known that the screening RF axial current flows mainly near the boundary. This distribution of the Joule heating would lead to a flat temperature profile if the dominant energy loss mechanism is heat conduction. The observed hollow temperature distribution shows that the dominant energy loss mechanism is line radiation. The positions giving the peaked density are inside the field null position evaluated from the profiles of the axial field. The fact may indicate the plasma pressure does not sustain only by the reversed magnetic field.

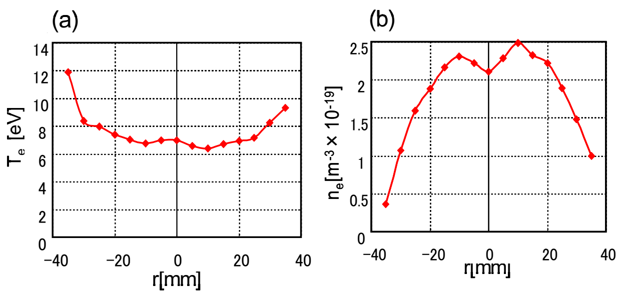

Fig.8 (a) Radial profile of electron density, and (b) electron temperature at z=0

Figure 9 shows the radial distribution of the plasma pressure $p=n_i kT_i+n_e kT_e \cong n_e kT_e$ (assuming $T_i<<T_e$) plus the axial magnetic field pressure $B_z^2/2\mu_0$ and the θ and time averaged pressure of θ-component of the RMF, i.e. $(B^2_{\theta A\text{-}A'}+B^2_{\theta B\text{-}B'})/8\mu_0$, where $B_{\theta A\text{-}A'}$ and $B_{\theta B\text{-}B'}$ are the θ-component of the RMF along the lines A-A' and B-B', respectively. The curve shown by D is fairly flat except outermost points. The flat distribution proves that the radial pressure are balanced and the θ-component of the RMF pressure mainly supports the plasma pressure.

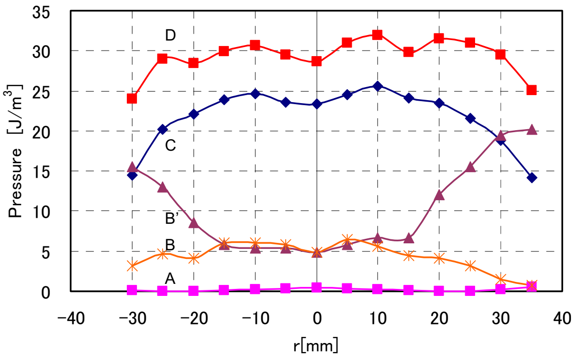

Fig.9 Radial pressure profiles. A corresponds the axial magnetic field, B and B' the θ-components of RMF on the line A-A' and B-B' in Fig.4, C the plasma pressure, and D the sum of the plasma pressure and the magnetic pressures.

4. Summary and Conclusions

Experiments of the formation and the sustenance of an FRC for 40msec by the RMF have been carried out. The FRC with a density $2.2\times10^{19}m^{-3}$ and an electron temperature 7 to 12eV is formed by applying an RMF through a glass chamber filled with Argonne gas of 10 Pa. without pre-ionization. The separatrix radius and length are identified by a magnetic probe. The current about 1kA is driven by the RMF. The antenna current decays due to the limited capacitance in the power supply during 40msec discharge. The FRC is gradually getting smaller in both length and radius, but still maintained after 40msec. Just after an RMF is applied, the antenna currents are reduced about a half because the vector potential induced by the RMF increases the resistance of an antenna and also makes the circuit out of tune due to the decreased inductance of the antenna.[14] The RMF, however, still deeply penetrates into the plasma. The reversed axial magnetic field is observed to fluctuate for the initial period of 15msec and make a transition into a quiet phase. Some relaxation process may occur during the fluctuation.[12]

In the other experiments [2-7], the magnitude of the RMF is smaller than the axial magnetic field. The RMF did not penetrated deeply into the center during the discharge and gave the theoretical interpretation of partial penetration.[6] Since the amplitude of the RMF in this experiment, however, is much larger than that of the axial magnetic field. The present experimental result has revealed a full penetration of the RMF when the magnitude of the RMF is strong enough.

The electrons are proved to rotate synchronously with an RMF except for near the chamber wall. The plasma current is roughly estimated to be $j_p=-en_er\omega\approx10^5A/m^2$ (r=0.02 m) at t=20msec neglecting the ion cancel current, which roughly agrees with the currents calculated by the axial magnetic field measurement shown in Fig.7. The reversed magnetic field is too weaker to sustain the plasma pressure. The radial profile of a time-averaged RMF pressure is concave or convex depending on the RMF phase. Both of the RMF pressures exert alternately the force. The concave pressure is stronger than the convex one, the plasma receives the net inwards force on average. The θ-component of the RMF plays a major role of radial pressure balance in the present experiment. No macro-instability is observed for the long duration 40msec. The large amplitude of the RMF also may exert the stabilizing effects on the FRC.

Acknowledgment

The authors acknowledgment Dr. K. Kitano (Osaka Univ.) for his invaluable suggestion in constructing the Kansai Rotamak device.

5. References

[1] H.A. Blevin and P. C. Thoneman, Nucl. Fusion Suppl. Part 1,**55** (1962).
[2] W.N. Hugrass, I.R. Jones and M.G.R. Philiiips, J. Plasma Phys., **26**, 465-480 (1981).
[3] H.Y. Guo, A.L. Hoffman, R.D. Brooks, A.M. Peter, Z. A. Pietrzyk, S.J. Tobin, and G. R. Votroubek, Physics of Plasmas, **9**, 185 (2003).
[4] W.N. Hugrass and M. Ohnishi, Plasma Phys. Control. Fusion **41**, 955 (1990).
[5] I.R. Jones, Phys. Plasmas **6**, 2771 (1999).
[6] A.L. Hoffman, H.Y. Guo, K.E. Miller and R.D. Milroy, Nuclear Fusion **45**,167 (2005).
[7] H.Y. Guo, A.L. Hoffman and R.D. Milroy, Phys. Plasmas **14**,112502 (2007).
[8] R.D. Milroy, Physics of Plasams, **6**, 2771 (1999).
[9] R.G. Storer, Plasma Physics **24**, 543 (1982).
[10] W.N.Hugrass, J. Plasma Phys., **28**, 369 (1982).
[11] R.G. Storer, Nuclear Instruments and Methods in Physics Research, **207**, 135 (1983).
[12] L. Steinhauer, Phys. Plasmas **8**, 3367 (2001).
[13] W.N. Hugrass, Aust. J. Phys. **38**,157 (1985).
[14] W.N. Hugrass, T. Okada and M. Ohnishi, Plasma Phys. Control. Fusion,**50**,055008（2008）.